Physics and applications of photonic nanocrystals

Ekmel Ozbay*, Kaan Guven and Koray Aydin

Department of Physics, Bilkent University,
Bilkent 06800, Ankara, Turkey
E-mail: ozbay@fen.bilkent.edu.tr
*Corresponding author

Mehmet Bayindir

Research Laboratory of Electronics,
Massachusetts Institute of Technology,
Cambridge, MA 02139-4307, USA

Abstract: Photonic nanocrystals are periodic dielectric or metallic structures having photonic bands in analogy to electronic bands of semiconductors. The presence of photonic band-gaps, where the propagation of photons of certain frequencies is prohibited, and the variety of photon dispersions give rise to novel and unusual optical phenomena. Consequently, photonic crystals are now envisaged as an essential building block of future photonic devices. This paper aims to provide a review of contemporary developments on the physics and applications of photonic crystals with an emphasis on optical properties of coupled microcavity waveguides and on the negative refraction phenomenon. The enhancement of spontaneous emission in a silicon nitride photonic nanocrystal is investigated in detail. Both the negative refraction of a Gaussian beam and the focusing of a microwave point source through a photonic crystal slab with subwavelength resolution are studied experimentally.

Kaan Guven was born in Izmir, Turkey in 1971. He obtained BS (1993), MS (1995), and PhD (1999) degrees in physics from Bilkent University. During his Ph.D., he worked on the many-body interactions in low dimensional electron-hole systems. In 1999, he joined the group of Prof. Klaus Von Klitzing at Max-Planck Institut in Stuttgart, Germany as Postdoctoral Associate. He is Visiting Assistant Professor in Bilkent University since 2002, working on photonic band gap materials and metamaterials.

Koray Aydin was born in Ankara, Turkey in 1980. He received his BS degree in Physics from Bilkent University. He started his MS study in 2002 at the Department of Physics, Bilkent University. He is working on negative refraction properties and characterisation of metamaterials.

Mehmet Bayindir was born in Konya, Turkey, in 1975. He received his BS (1995), MS (1997), and PhD (2002) degrees in Physics from the Bilkent University, Ankara, Turkey. During his PhD he worked with Prof. Ekmel Ozbay on photonic band gap materials. He was the recipient of the New Focus Award of the Optical Society of America in 2001. In 2002, he joined the photonic band gap group in MIT as Postdoctoral Associate. He is working on microstructured fibers and photonic band gap materials.

1   Introduction

The last decade marks the start of a new research field of the so-called photonic crystals (PC) [1,2]. These periodic dielectric or metallic structures have photonic bands which exhibit arbitrarily different dispersions for the propagation of electromagnetic waves, and band gaps, where the propagation is prohibited at certain range of wavelengths. In this respect, there is a close analogy between a photon in a photonic crystal, and an electron in a semiconductor. Based on these properties, photonic crystals provide a medium where the propagation of light can be modified virtually in any way in a controllable manner. Their application potential covers the existing electromagnetic technologies for improvement, and extends beyond for advancement. From fundamental physics point of view, photonic crystals provide access to novel and unusual optical phenomena [3–5].

In particular, development of three-dimensional (3D) and two-dimensional (2D) photonic crystals in micro- and nanoscale are under deep scrutiny, because they reside in the realm of telecommunication and optical wavelengths [6–11]. Maxwell's equations are scale invariant, but keeping the structural uniformity while scaling the photonic crystal down to optical wavelengths is still a challenging problem, especially for three dimensional photonic crystals. Numerous fabrication techniques have been investigated in the last decade. Kuramochi et al. proposed alternating layer deposition and etching process for fabrication of 3D photonic crystals [12]. Baba and Matsuzaki studied the fabrication and photoluminescence of InGaAsP/InP 2D photonic crystals [8]. Sugimoto et al. [13] fabricated and characterised 2D AlGaAs photonic crystal slabs by electron lithography in combination with dry etching. In terms of dimensionality, 2D and 1D counterparts are more feasible to fabrication by existing techniques but they may suffer from diffraction losses along the unconfined spatial directions [14–16]. Yet, these losses can be reduced significantly by index guided [17] or again 2D photonic crystal based [18] cladding layers in the perpendicular (out of propagation plane) direction.

In this paper, we review certain optical properties and applications of photonic crystal structures. Our aim is twofold:

- to investigate the improvement that photonic crystals provide for a typical well known optical process, namely the spontaneous emission

- to demonstrate novel optical phenomena that occur by means of photonic crystals, namely the negative refraction.

The paper is organised as follows: In the first part we consider the optical properties of coupled micro-cavity waveguide (CMCW) structures in one-dimensional photonic crystals. The dispersion and group velocity of photons within the guided band are investigated briefly within tight-binding formalism of coupled localised cavity modes. The utilisation of CMCWs is demonstrated by a structure which enhances the spontaneous emission significantly. In the second part, experiment and simulation of a dielectric based two-dimensional photonic crystal slab are presented, which exhibits negative refraction and unusual focusing properties. The last section summarises the paper and gives some concluding remarks.

2   Coupled micro cavity waveguide structures in 1D photonic crystals

One-dimensional (1D) spatially periodic, quasiperiodic, and random photonic bandgap (PBG) structures have been studied extensively. Two major reasons for this interest are: (i) that the lack of confinement in two spatial directions does not hinder the investigation of certain optical phenomena and (ii) that the structures can be fabricated much easier compared to their higher dimensional counterparts.

As a result, many studies concerning these structures are reported in recent years. Localisation of light in disordered and quasi periodic photonic systems are widely studied [19,20]. Superluminal tunnelling through 1D PBG materials has also inspired great interest [21–23]. Properties of metallic-dielectric 1D PBG structures are investigated [24–27]. By using 1D PBG structures, potential applications concerning nonlinear optical phenomena were reported such as second harmonic generation [28], pulse compression [29], optical limiting and switching [30,31], filters [32,33], and photonic band edge lasers [34]. Moreover, the modification of spontaneous emission from atoms placed in 1D photonic band gap structures has been demonstrated [35–39]. Similar studies were carried out in two-dimensional photonic crystals involving light emitting diodes [40,41], and photonic crystal based lasers [42,43].

By introducing a defect into a PBG structure, it is possible to obtain highly localised cavity modes inside the photonic band gap, which is analogous to the impurity states inside the semiconductor band gap [44]. Since high quality cavities have a crucial role in most of the photonic crystal based applications, investigation of the optical properties of cavities is essential. In recent years, coupled-microcavities have been investigated [45], and used in various applications [38,39,46,47]. These structures consist of two or more planar Fabry-Perot microcavities which are coupled to each other.

Theoretical analysis of CMCs is formulated within the framework of tight binding (TB) approximation [48] via the analogies drawn between the Schrödinger equation and the classical electromagnetic wave equation [49–54]. By using direct implications of the TB picture, a novel propagation mechanism for photons through localised coupled cavity

modes in the photonic crystals was proposed [50,53] and demonstrated [54,55] in three-dimensional photonic crystals at microwave frequencies.

In this section, we present the experimental demonstration of guiding light through a CMC structure of Si_3N_4/SiO_2 (silicon nitride/silicon-oxide) layers with $\lambda/2$ SiO_2 cavity layers (see Figure 1 for schematic representation). The layers were deposited on glass substrates by plasma enhanced chemical vapour deposition (PECVD) at 250°C [56]. Nitrogen (N_2) balanced 2% silane (SiH_4), pure ammonia (NH_3) and nitrous oxide (N_2O) were used as the silicon, nitride and oxide sources, respectively. The cavities are introduced by doubling the deposition time of the silicon-oxide layers. The thicknesses are chosen as $d_L = 100$ nm and $d_H = 70$ nm for SiO_2 and Si_3N_4 layers and 200 nm for the cavity layers.

Figure 1   Propagation of photons by hopping through localised coupled-cavity modes illustrated. Bottom figure represents the multilayer CMC structure composed of $\lambda/4$ SiO_2 and Si_3N_4 pairs with SiO_2 layers
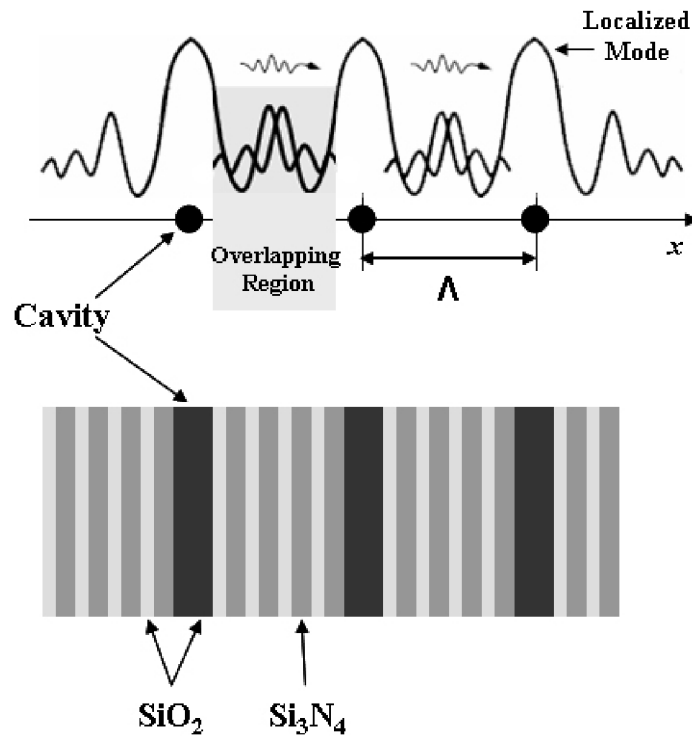
Figure 2 shows the measured and calculated (by transfer matrix method) transmission spectra of fabricated samples with intercavity distances, $\Lambda_A = 2.5$, $\Lambda_B = 3.5$ pairs. Nearly 100% transmission is observed throughout the guiding band which extends from 540 nm to 627 nm for sample A and from 554 nm to 610 nm for sample B. The experimental results are in good agreement with the Transfer Matrix Method (TMM) simulations. The minimum value 0.1% of the measured transmission is limited by the experimental set-up.

Figure 2 Measured (solid lines) and calculated (dotted lines) transmission spectra of CMC structures with intercavity distance $\Lambda_A = 2.5$ (top) and $\Lambda_B = 3.5$, respectively
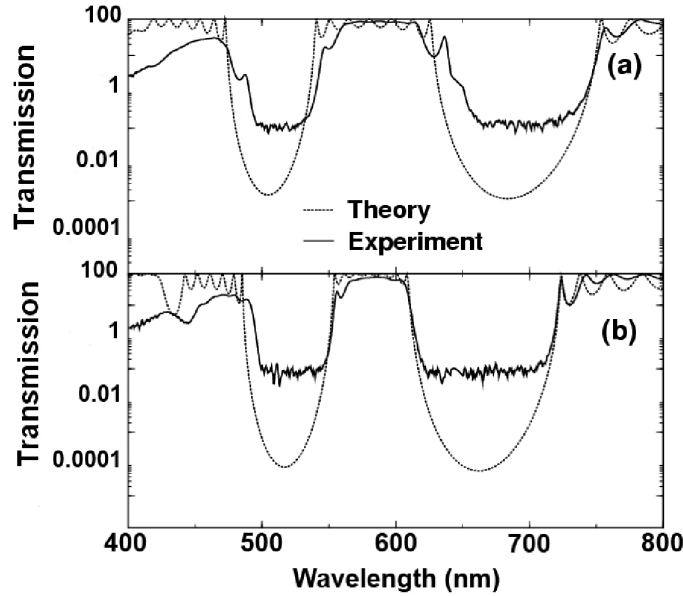
Within the TB approximation, dispersion relation, group velocity, and photon lifetime can be characterised by a single coupling parameter κ [50,53]. For the present structures, it is found that $\kappa \approx 0.067$ from the splitting of two coupled cavities, and is consistent with the result that is obtained from bandwidth of the guiding band [57]. The dispersion relation of the CMC is given by [50,53,54]

$$\omega_k = \Omega[1 + \kappa \cos(k\Lambda)] , \tag{1}$$

where $\Omega = 517.4$ THz is the measured single-cavity resonance frequency [58]. The group velocity and lifetime of photons follows from this relation as

$$v_g = \nabla_k \omega_k = -\kappa \Lambda \Omega \sin(k\Lambda) \quad \tau_p = \frac{L}{v_g} + \frac{2\pi L}{c} \tag{2}$$

where L is the total thickness of the structure. Figure 3 shows the calculated parameters using experimentally determined coupling constant. It should be emphasised that the group velocity at the guiding band center is one order of magnitude smaller than that of light in vacuum, and decreases drastically at the edges. Since smaller group velocity enhances optical processes, this property, combined with efficient transmission through coupled cavity waveguides brings important advantages to optical applications as will be discussed by an example in the next section.

Figure 3 (a) Calculated dispersion relation (Eq. 1) for sample A using measured coupling
parameter $\kappa \approx 0.067$. (b) Normalised group velocity and (c) photon lifetime as a
function of wavevector k. Notice that $v_g \rightarrow 0$ and $\tau_p \rightarrow \infty$ at the edges of the guiding
band.
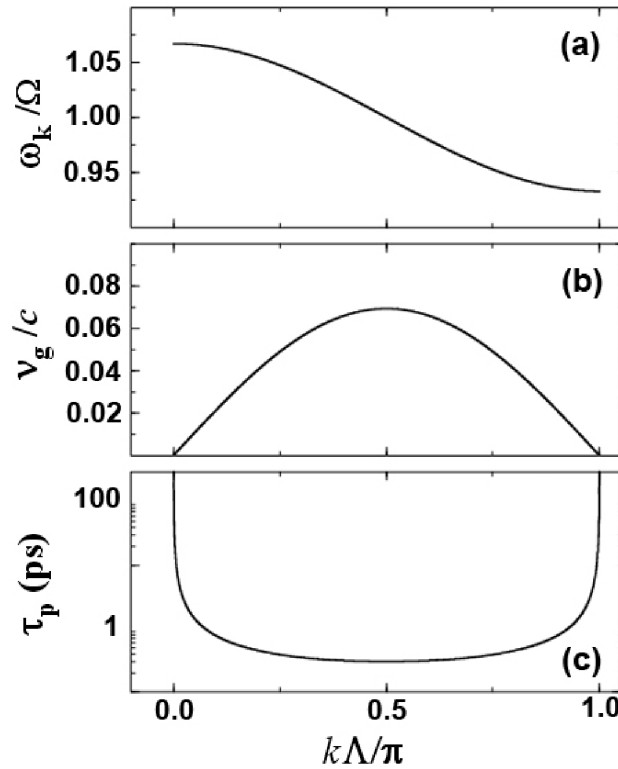
2.1 *Enhancement of spontaneous emission through coupled cavity waveguides in 1D photonic micro- and nanocrystals*

Many optical applications demand the ability to control the spontaneous emission for
inhibition or enhancement. Since the density of electromagnetic modes $\rho(\omega)$ is modified
by the surrounding environment, the spontaneous emission from atoms can be controlled
by placing the atoms inside cavities [35,36,45,46,59–67]. Fermi's Golden rule states that
the spontaneous emission rate is directly proportional to the photon density of modes:
$\Gamma_s \sim \rho(\omega) \sim v_g^{-1}$ [35]. From this point of view, cavity structures in photonic band gap
materials provide a convenient medium where the density of photon modes can be altered
locally. By constructing a coupled cavity structure inside a photonic crystal, a
transmission band inside the photonic band-gap opens. As demonstrated in the preceding
section, the group velocity tends to zero and the photon lifetime increases drastically at
the edges of the transmission band. Thus, it is expected that the spontaneous emission
from a coupled microcavity structure can be enhanced and this enhancement can be
transferred across the structure without a significant loss. In addition, the position and
width of the guiding band can be adjusted at fabrication phase by changing the thickness
of the cavity layers and the intercavity distance, respectively. Here, we present an
experimental study of the modification of spontaneous emission from the hydrogenated

amorphous-silicon-nitride active layers in a Fabry-Perot (FP) resonator and a coupled-microcavity structure [38,39].

We refer the reader to the previous section for the fabrication details of the CMC structures. Figure 4 shows the schematic drawing of the sample structure and experimental setup. The refractive indices and thicknesses of layers were $n_{SiO2} = 1.46$, $n_{Si3N4} = 1.98$, $d_{SiO2} = 124.8$ nm, and $d_{Si3N4} = 92.0$ nm. The $\lambda/2$ $d_{cavity} = 184$ nm cavities were deposited with an intercavity distance $\Lambda = 4.5$ pairs.

Figure 4 Schematic of the coupled-microcavity structure and the experimental setup for measuring the photoluminescence spectra.
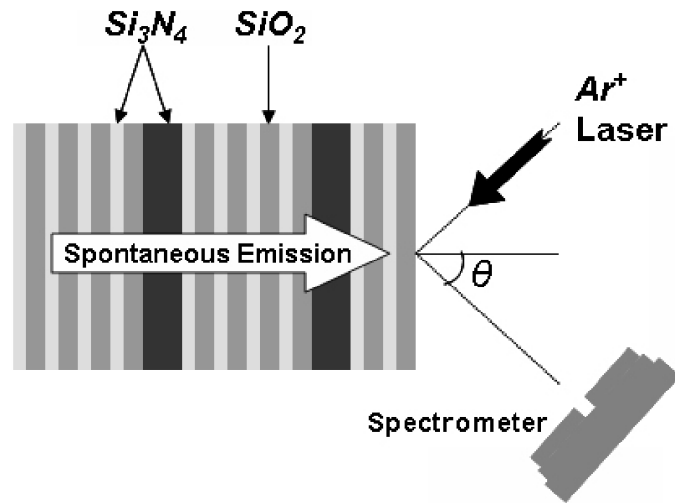
The room temperature photoluminescence (PL) measurements were performed using a 1-m double monochromator, equipped with a cooled GaAs photomultiplier tube and standard photon counting electronics, at $\theta = 0°$ with respect to the surface normal and with a spectral resolution of 2 nm. An Ar^+ laser operating at 488 nm with 120 mW output power was focused with a 15-cm focal-length cylindrical lens on the sample. The transmission spectrum is obtained by a fiber spectrometer.

We first present the results for a single cavity structure: Figure 5a shows the measured overall transmission spectrum of a single Fabry-Perot microcavity which consists of 16 pairs of $\lambda/4$ thick Si_3N_4/SiO_2 layers and a $\lambda/2$ thick Si_3N_4 cavity layer. Comparison of the PL spectra of the FP microcavity (solid line) and a single Si_3N_4 layer (dotted line) shows that the narrow-band PL peak at $\lambda = 722$ nm is enhanced drastically in the presence of the FP structure (Figure 5b). Note that the PL spectrum of single Si_3N_4 layer was multiplied by a factor of five for visibility. Similar observations were reported in [36] and [37]. In the angular distribution of the PL spectra, the resonance peak exhibits a slight blue-shift, and the peak intensity decreases rapidly with increasing angle (Figure 6).

Figure 5 (top) Transmission spectrum of a hydrogenated amorphous-silicon-nitride Fabry-Perot structure with a single microcavity. (bottom) Cavity mode enlarged. At peak wavelength, the PL intensity is enhanced by ~12x relative to a thin film structure of the same material

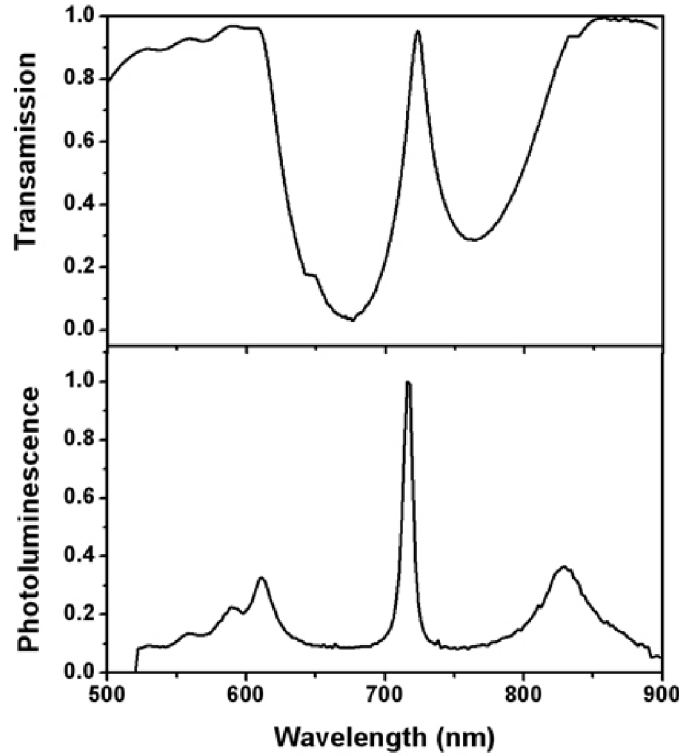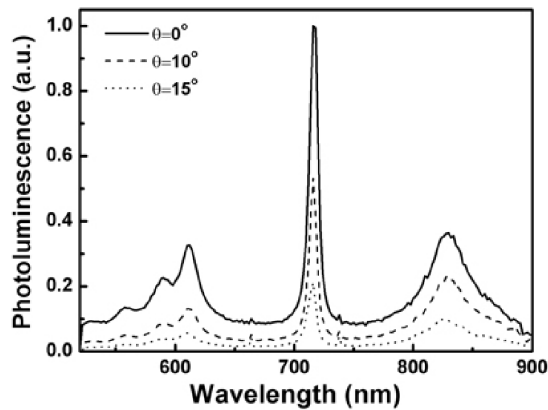

Figure 6 Angular distribution of the photoluminescence intensity of a single microcavity as a function of wavelength

In the case of a CMC structure having 36 pairs of Si_3N_4/SiO_2 and four Si_3N_4 cavity layers (see Figure 4a for the schematic), nearly 100 percent transmission is achieved throughout the CMC band. This is in agreement with the calculated transmission spectrum using

transfer matrix method (Figure 7a). The measured PL spectrum shows an overall enhancement of the spontaneous emission across the transmission band of the coupled-cavity structure extending from 690 to 770 nm, particularly at the lower edge of the band (Figure 7b). Enhancement effects are also reported at the photonic band edges [35].

Figure 7 (a) Comparison of the measured (solid line) and calculated (dotted line) transmission through the Si_3N_4/SiO_2 coupled-microcavity (CMC) structure. (b) Measured photoluminescence spectrum of the CMC structure
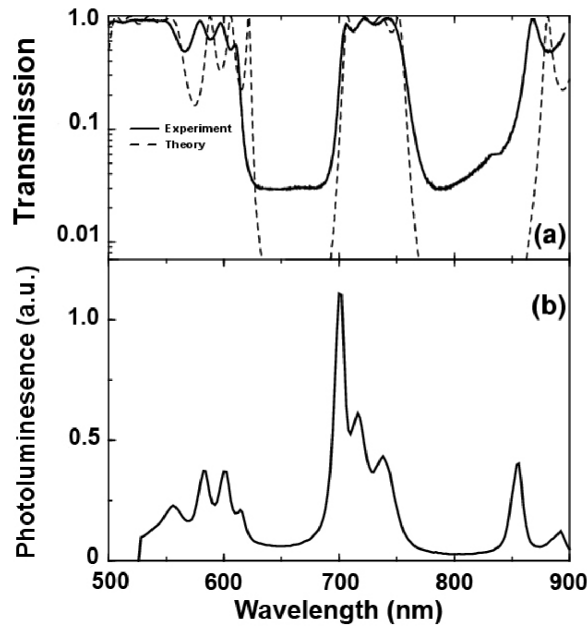
In the next section we start to discuss novel optical phenomena that can be observed in photonic crystal structures.

3 Negative refraction and point focusing using photonic crystal superlens

The refraction of light in the 'wrong' way is intuitively associated with the presence of a medium possessing negative index of refraction as proposed by Veselago in the 1960s [68]. However, no natural material is known to exhibit this property up to date. Almost four decades after its introduction, this idea has been revived by recent contributions which proposed the realisation of these materials, albeit in an artificial manner [69–75]. The possibility of a negative index of refraction has been described in the context of an effective-medium theory. Two periodic metallic structures with frequency dependent permittivity and permeability respectively, may have an overlapping frequency range where the permittivity and the permeability take negative values with vanishing imaginary parts. When these materials joined to form a composite meta-material, an effective medium with negative index of refraction may occur. These ideas are pursued with a growing interest along with an intense debate about whether these

composite structures can be described as truly negative refractive index materials or not [76–78].

In the mean time, photonic crystals joined the quest for the realisation of negative refraction without resorting to the use of negative refractive index materials. Theoretical works indicate that the band structure of photonic crystals exhibits unusual dispersion of the electromagnetic waves including the possibility of negative group velocity, which can be regarded as a negative effective index of refraction, similar to the negative effective mass of electrons in a semiconductor. Negative refraction and large beam steering, called 'super prism phenomenon', at the interface of a 3D photonic crystal has been experimentally observed [3]. Notomi [79] studied light propagation and refraction phenomenon in strongly modulated 2D photonic crystals. Gralak et al. [80] reported on the anomalous refractive properties of photonic crystals. Luo et al. [81] investigated and proposed the conditions for all angle negative refraction through a photonic crystal and superlens phenomenon. Foteinopoulou et al. [82] demonstrated the negative refraction at the photonic crystal interface with negative refractive index using finite difference time domain simulations.

We recently reported on the experimental investigation of negative refraction and subwavelength focusing of microwaves in a 2D photonic crystal structure consisting of a square array of dielectric rods in air [4]. The dielectric constant of the rods is $\varepsilon = 9.61$, with a diameter of 3.15 mm, and length of 150 mm. The lattice constant is a = 4.79 mm. Propagation properties of the electromagnetic wave within the crystal can be described by studying isofrequency contours in *k*-space. The transverse magnetic (TM) polarised valence band of the photonic crystal calculated by plane wave expansion method, is shown in Figure 8(a). Following the analysis of [81], the scaled frequency range that gives negative refraction for the present structure extends from $\tilde{\omega} = 0.2093$ to $\tilde{\omega} = 0.2467$. Negative refraction requires convex EFSs for the PC, that are larger than the EFSs for air. The EFSs for air and PC at $\tilde{\omega} = 0.2189$ are shown in Figure 5(b). Note in the figure that conservation of surface-parallel wave vector gives the direction of the refracted waves inside the PC.

Figure 8   (a) Band diagram for our structure for TM polarisation. Negative refractive region is shaded. (b) Frequency contours of air and PC at $\omega a/2\pi c = 0.2189$ ($f = 13.698$ GHz). Here θ denotes the incidence angle from air to PC
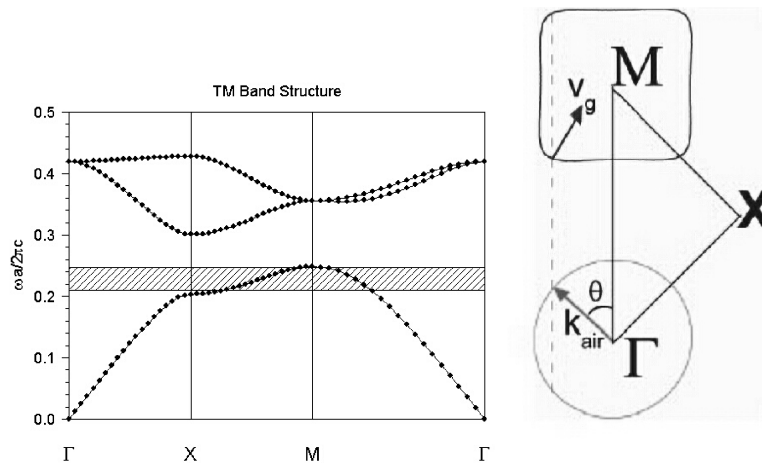
The verification of the predicted negative refraction is performed by an experimental setup which consists of an HP 8510C network analyser, a horn antenna as the transmitter and a monopole antenna as the receiver (Figure 9). The incidence normal to interfaces extends along the ΓM direction of the PC. In all measurements and simulations the electric field is kept parallel to the rods. The horn antenna is oriented such that the incident waves make an angle of $45°$ with the normal of ΓM interface. The operating frequency is selected as $\tilde{\omega} = 0.2189$. As explained later, the structure exhibits the maximum angular range of negative refraction at this frequency. The spatial distribution of the time averaged incident field intensity along the 'front' (air-to-PC) and 'back' (PC-to-air) interface locations are measured first in the absence of and then by placing the PC. For a direct comparison of theoretical predictions and experimental results, simulation of the structure based on experimental parameters using a finite difference time domain (FDTD) method is performed. Figure 10a summarises the measured and simulated spatial distributions of intensity at the interfaces for the PC. The center-to-center shift of the outgoing beam relative to incident beam towards the left side clearly indicates the occurrence of negative refraction. For comparison purposes, the measurements and the simulations are repeated with a slab that contains only polystyrene pellets, which has a refractive index of 1.46. As can be seen in Figure 10b, the refracted beam is now on the right hand side of the incident beam. The positive refractive index determined from the experiment is 1.52, which is close to the tabulated value of 1.46.

Figure 9   Schematics of the experimental setup. For refraction measurements a transmitter horn antenna and a receiver monopole antenna is used. For focusing experiment both the transmitter and receiver are monopole antennas
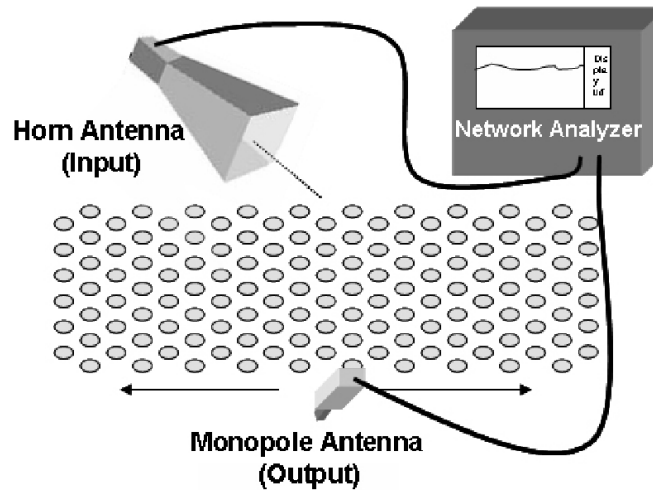
Figure 10 Comparison between negative (a) and positive refraction (b). (a) Thin solid curves
denote the simulated average intensity at the second interface with PC (black) and at the
first interface without PC (grey). Measured power at the second interface with PC
(black dots) and at the first interface without PC (grey dots). (b) Simulated average
intensity at the second interface with a slab of polystyrene pellets (solid black curve)
and at the first interface without slab (solid grey curve). Measured power distribution at
the second interface with slab (black dots) and at the first interface without slab
(grey dots). (c) Schematics of positive and negative refraction

(a)

(b)

(c)
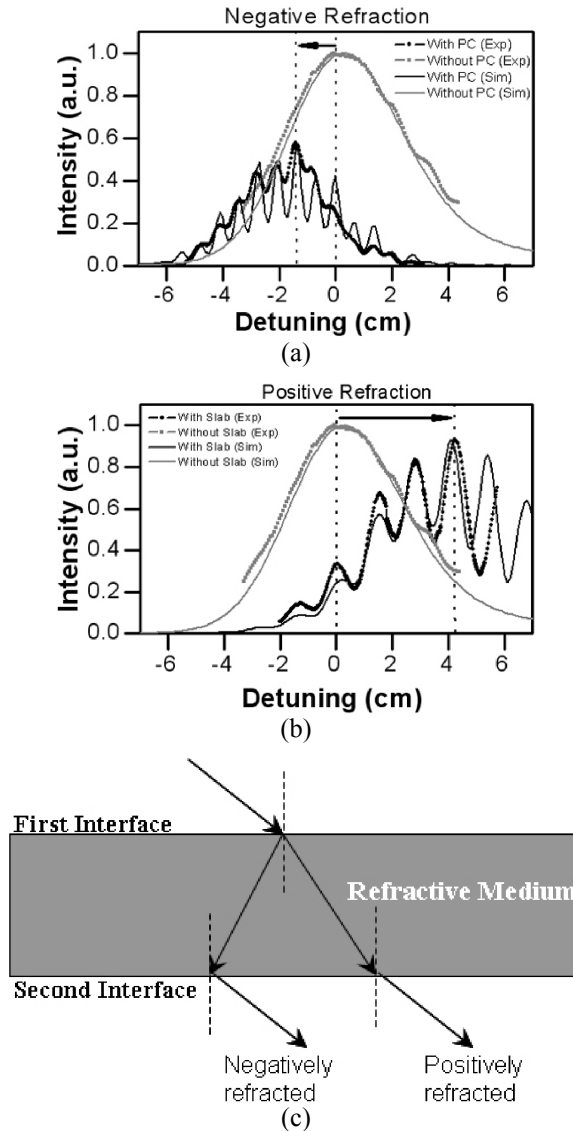
For the selected frequency, the incident field couples to the first band and propagates
according to its dispersion. The advantage of the first band is that since $\lambda > 2\sqrt{2}\,a$ the
propagation does not suffer from Bragg reflections that take place inside the photonic
crystal and we have a well defined single beam propagation. For this reason Snell's law

may be applied to the PC as $n(f, \mathbf{k_i}) \sin \theta_r = n_{air} \sin \theta_i$, where θ_i is the angle of incidence, θ_r the angle of refraction, and $n(f, \mathbf{k_i})$ is the frequency dependent, anisotropic refractive index along the propagation direction $\mathbf{k_i}$. Based on this equation, the negative index of refraction determined from the experiment is -1.94 which is very close to the theoretical value of -2.06 calculated by the FDTD method. Note also the 63% transmission at this frequency provided by the first band which is almost three orders of magnitude larger than the typical transmission in a left handed material [71,74].

In the aforementioned frequency range the EFCs are square shaped around the M point in the Brillouin zone (Figure 8b). Figure 11 shows the resulting anisotropy of $n(f, \mathbf{k_i})$, at $\tilde{\omega} = 0.2189$ ($f = 13.698$ GHz) that is determined for various angles of incidence. Negative refraction behaviour is observed for the incidence angles $>20°$. In this angular range $\mathbf{v_g} \, \mathbf{k_{i\parallel}} < 0$, (while $\mathbf{v_g} \, \mathbf{k_i} > 0$), where $\mathbf{v_g}$ is the group velocity inside the PC that is given by $\nabla_k \omega(k)$ and $\mathbf{k_{i\parallel}}$ is the component of wave vector, incident from air to the PC, which is parallel to the interface. At 13.698 GHz, the respective EFCs for air and for the PC have almost the same diameter which maximises the angular range of negative refraction for this structure (Figure 8b). If a higher frequency is used, the EFS for air will be larger than the EFS for the PC. In such a case, the maximum angle where we obtain negative refraction gets smaller due to total internal reflection. This results in a narrower angle range for the negative refraction behaviour. If a lower frequency is used, we then have EFS for air that is smaller than the EFS for the PC. This in turn increases the minimum angle where we obtain negative refraction, which again reduces the angle range for the negative refraction behaviour.

Figure 11 Measured (diamonds) and calculated (solid curve) angle of refraction versus angle of incidence dependence at 13.698 GHz
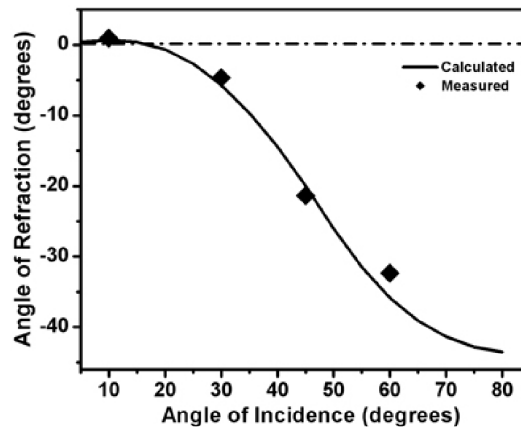
Perhaps the most controversial issue involving negative refraction induced phenomena is superlensing [83–87]. Ideally this requires an isotropic index of refraction with a value of -1 and the amplification of evanescent field modes while propagating across the lens structure in order to contribute to the image formation on the focal plane. Anisotropy and deviations from negative unity will result in an impaired focusing, but still exhibit unusual focusing properties in contrast to positive refractive index materials. In order to investigate this phenomenon, we use the optimum frequency for negative refraction to

cover a broad angular range. The constructed PC has 15 layers in the propagation direction and 21 layers in the lateral direction. Finite difference time domain (FDTD) simulations with experimental parameters predict the formation of an image at 0.7 mm away from the PC-air interface for a point source that is placed at 0.7 mm away from the air-PC interface. To show the focusing on the image plane in the vicinity of the PC, the distribution of time averaged intensity along the image plane with and without the PC are calculated (Figure 12). In the experiment, a monopole antenna is used as the point source (Figure 9). The power distribution at the image plane is measured by scanning the transmitted field intensity along the image plane. The measured distribution is also shown in Figure 12. The full width at half maximum (FWHM) of the measured focused beam is found to be 0.21λ, which is in good agreement with the calculated FWHM. The calculated FWHM of the beam at this plane in the absence of the PC is found to be 5.94λ. This implies an enhancement of the transmitted field about 25x compared to free space. We stress the point that the narrow incidence angle range for negative refraction (<20°) and the anisotropy restricts the position of the source in the vicinity of the crystal surface for proper observation of focusing effect. The observed subwavelength focusing can be explained by recent theoretical work of Luo et al [89]. As described in this reference, the subwavelength imaging is possible due to the amplification of evanescent waves through the photonic crystal. They have also found out that the periodicity of the photonic crystal imposes an upper cutoff to the transverse wave vector that can be amplified, which brings an ultimate limit to the superlens resolution. Within this description, we can also introduce an upper limit on the location of the source from the PC. As the evanescent waves have to reach the surface of the PC (before they decay out), the source has to be close enough to the PC. In that sense, the theoretically predicted and the experimentally observed subwavelength resolution in PCs will be limited to the cases where the source is close to the PC.

Figure 12 Focusing: Measured power distribution (dots) and calculated average intensity (solid curve) at the image plane. Full width at half maximum of the measured image is ~0.21λ. Spatial power distribution without PC is also shown (dotted thin line)
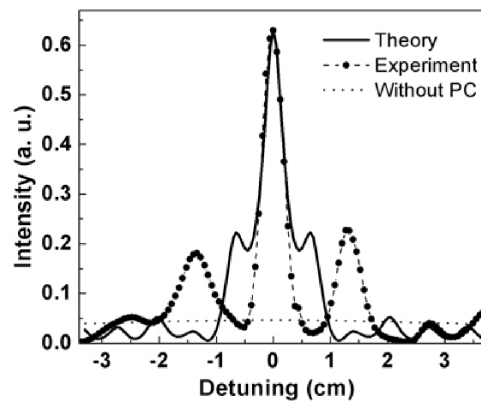
In order to investigate the subwavelength resolution, we use the same photonic crystal structure and first consider two coherent sources which are separated by a distance of ≈λ/3 and placed 0.7 mm away from the photonic crystal interface. Figure 13a shows the lateral profile of the transmitted power 0.7 mm away from the second interface. There's a

good agreement between the simulated and measured data. When the crystal is removed, no features are visible on the power profile (dashed line). To exclude interference effects due to coherence, we repeat the experiment using two incoherent point sources having frequencies 13.698 GHz and 13.608 GHz respectively. Independent signal generators are used for driving the monopole antennas to ensure incoherent behavior, and a powermeter is used for measurement. The measured and simulated power distribution in the presence of photonic crystal 0.7 mm away from the second interface is shown in Figure 13b. The peaks corresponding to the incoherent source pair are resolved. One can argue that the observed enhanced resolution can be attributed to the high refractive index as in the case of oil (or solid) immersion microscopy. In this case, higher wave vectors which are evanescent in air can transmit through the crystal and form a near-field image with subwavelength resolution. In order to check this possibility, the incoherent source setup was simulated for a uniform dielectric slab with a high refractive index. The dashed lines in Figure 13b indicates the power distribution in the presence of a dielectric slab of $n = 3.1$ and $n = 15$, respectively. Note that $n = 3.1$ is also the refractive index of the alumina rods used in constructing the photonic crystal. Even in the case of dielectric slab with artificially high refractive index ($n = 15$), the resolution of the sources are not present. Besides, the large reflection due to high index contrast at the interface significantly reduces the transmitted power when compared to the high (63%) transmission obtained from the photonic crystal at this operating frequency. So, even if the observed subwavelength is associated with near field effects, this is not achievable by ubiquitous materials.

Figure 13 Subwavelength resolution: **(a)** Measured (dots) and simulated (solid curve) power distribution of two coherent sources separated by $\approx\lambda/3$ at 0.7 mm away from the second interface. Dashed line denotes the calculated average intensity in the absence of photonic crystal **(b)** The same setup with two incoherent point sources. Experiment (dots) and simulation (solid line) shows that the peaks are resolved. The lower dashed and dot-dashed curves indicate the power distribution for uniform dielectric slabs with refractive indices $n = 3.1$ and $n = 15$, respectively. Note the scaling of the power corresponding to high index slab
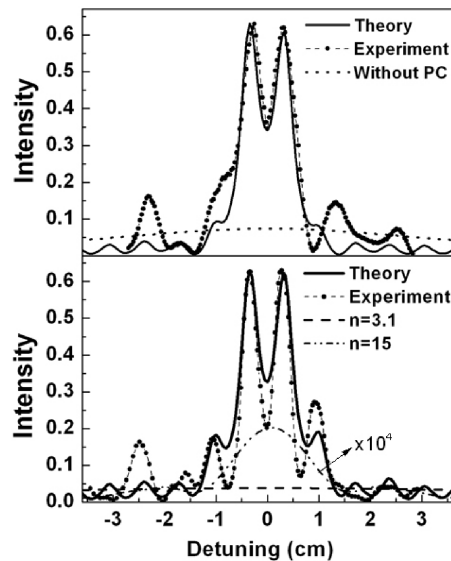
The negative refraction and focusing effects reported here depend solely on the dielectric constant of the materials and on the geometrical parameters of the photonic crystal. Using transparent semiconductors with refractive indices similar to that of presented here, it may be possible to observe these effects in optical wavelengths just by scaling the structures. In this respect, photonic crystals are superior to metal based composite materials mentioned at the beginning of this section because increased absorption in metals puts severe limitations to the scaling of these structures towards the optical regime.

4   Conclusion

In this paper we discussed two features of photonic crystal structures. One of them is the enhancement (or inhibition) of spontaneous emission through coupled micro-cavity waveguides. This exemplifies how photonic crystals contribute to the control and advancement of existing optical processes and to their applications. The second feature is the negative refraction of electromagnetic waves through a photonic crystal slab. This unusual optical phenomenon may lead to applications such as photonic crystal based lenses with subwavelength focusing abilities. These examples also point out that the utilisation of photonic crystals can be scaled down or up across the entire electromagnetic spectrum, thus making them potentially available for a wide range of applications. Therefore, it would be a legitimate conclusion that photonic nano- and microcrystals will be an essential ingredient of future photonic integrated circuits.

References

1   Joannopoulos, J.D., Meade, R.D. and Winn, J.N. (1995) *Photonic Crystals: Molding the Flow of Light*, Princeton University Press, Princeton, NJ.

2   See papers in: Soukoulis, C.M. (Ed.) (2000) *Photonic Crystals and Light Localization in the 21st Century*, Kluwer, Dortrecht.

3   Kosaka, H., Kawashima, T., Tomita, A., Notomi, M., Tamamura, T., Sato, T. and Kawakami, S. (1998) 'Superprism phenomena in photonic crystals', *Phys. Rev. B*, Vol. 58, pp.R10096–R10099.

4   Cubukcu, E., Aydin, K., Ozbay, E., Foteinopoulou, S. and Soukoulis, C.M. (2003) `Negative Refraction by photonic crystals', *Nature*, Vol. 423, pp.604–605.

5   Parimi, P.V., Lu, T.W., Vodo, P. and Sridhar, S. (2003) 'Imaging by flat lens using negative refraction', *Nature*, Vol. 426, p.404.

6   Krauss, T., Song, Y.P., Thoms, S., Wilkinson C.D.W. and De La Rue, R.M. (1994) 'Fabrication of 2-D Photonic Band Gap Structures in GaAs/AlGaAs', *Electron. Lett.*, Vol. 30, No. 17, pp.1444–1446.

7   Gourley, P.L., Wendt, J.R., Vawter, G.A., Brennan, T.M. and Hammons, B.E. (1994) 'Optical properties of 2-dimensional photonic lattices fabricated as honeycomb nanostructures in compound semiconductors', *Appl. Phys. Lett.*, Vol. 64, No.6, pp.687–689.

8   Baba, T. and Matsuzaki, T. (1996) 'Fabrication and photoluminescence studies of GaInAsP/InP 2-Dimensional Photonic Crystals', *Jpn. J. Appl. Phys.*, Vol. 35, No. 2B, pp.1348–1352.

9   Prather, D.W., Murakowski, J.A., Venkatraraman, S., Peng, Y., Dillon, T. and Pustai, D. (2003) 'Enabling fabrication methods for photonic band gap devices', *SPIE Proc. 4984*.

10 Noda, S., Imada, M., Ogawa, S., Mochizuki, M. and Chutinan, A. (2002) 'Semiconductor three-dimensional and two-dimensional photonic crystals and devices', *IEEE J. Quant. Elect.*, Vol. 38, pp.726–735.

11 Lourtioz, J.M., Benisty, H., Chelnokov, A., David, S. and Olivier, S. (2003) 'Photonic crystals and the real world of optical telecommunications', *Ann. Telecomm.*, Vol. 58, Nos. 9/10, pp.1197–1237.

12 Kuramochi, E., Notomi, M., Kawashima, T., Takahashi, C., Takahashi, J., Tamamura, T. and Kawakami, S. (2000) 'Combination of nanolithography with alternating-layer deposition towards new class of photonic crystals', *Int. Workshop of Photonic and Electromagnetic Crystals*.

13 Sugimoto, Y., Ikeda, N., Carlsson, N., Asakawa, K., Kawai, N. and Inoue, K. (2002) 'Fabrication and characterization of different types of two-dimensional AlGaAs photonic crystal slabs', *J. Appl. Phys.*, Vol. 91, pp.922–929.

14 Baba, T. and Fukaya, N. (2001) 'Light propagation characteristics of defect waveguides in a photonic crystal slab', in Soukoulis M. (Ed.): *Photonic Crystals and Light Localization*, Kluwer Academic, Boston MA, pp.105–116.

15 Smith, C.J., Benisty, H., Olivier, S., Rattier, M., Weisbuch, C., Krauss, T.F., De La Rue, R.M., Houdré, R. and Oesterle, U. (2000) 'Low-loss channel waveguides with two-dimensional photonic crystal boundaries', *Appl. Phys. Lett.*, Vol. 77, pp.2813–2815.

16 Benisty, H., Weisbuch, C., Labilloy, D., Rattier, M., Smith, C.J.M., Krauss, T.F., De La Rue, R.M., Houdré, Oesterle, U., Jouanin, C. and Cassagne, D. (1999) 'Optical and confinement properties of two-dimensional photonic crystals', *J. Lightw. Tech.*, Vol. 17, No.11, pp.2063–2077.

17 Chow, E., Lin, S.Y., Johnson, S.G., Villeneuve P.R., Joannopoulos J.D., Wendt, J.R., Vawter, G.A., Zubrzycki, W., Hou, H. and Alleman, A. (2000) 'Three dimensional control of light in a two-dimensional photonic crystal slab', *Nature*, Vol. 407, pp.983–986.

18 Susa, N. (2003) 'Towards perfect vertical photonic band gap confinement in a photonic crystal slab', *Jpn. J. Appl. Phys.*, Vol. 42, pp.7157–7162.

19 Gellermann, W., Kohmoto, M., Sutherland, B. and Taylor, P.C. (1994) 'Localization of light waves in Fibonacci dielectric multilayers', *Phys. Rev. Lett.*, Vol. 72, pp.633–636.

20 Hattori, T., Tsurumachi, N., Kawato, S. and Nakatsuka, H. (1994) 'Photonic dispersion relation in a one-dimensional quasicrystal', *Phys. Rev. B*, Vol. 50, pp.R4220–R4223.

21 Nimtz, G. (1997) in Ranfagin, A. (Ed.): *Tunneling and its Implications*, World Scientific.

22 Spielmann, Ch., Szipocs, R., Stingl, A. and Krausz, F. (1994) 'Tunneling of optical pulses through photonic band gaps', *Phys. Rev. Lett.*, Vol. 72, pp.2308–2311.

23 Pereyra, P. (2000) 'Closed formulas for tunneling time in superlattices', *Phys. Rev. Lett.*, Vol. 84, pp.1772–1775.

24 Scalora, M., Bloemer, M.J., Pethel, A.S., Dowling, J.P., Bowden, C.M. and Manka, A.S. (1998) 'Transparent, metallo-dielectric, one-dimensional, photonic band gap structures', *J. Appl. Phys.*, Vol. 83, pp.2377-2383.

25 Bloemer, M.J. and Scalora M. (1998) 'Transmissive properties of Ag/MgF$_2$ photonic band gaps', *Appl. Phys. Lett.*, Vol. 72, pp.1676-1678.

26 Sibilia, C., Scalora, M., Centini, M., Bertolotti, M., Bloemer, M.J. and Bowden, C.M. (1999) 'Electromagnetic properties of periodic and quasiperiodic one-dimensional, metallo-dielectric photonic band gap structures', *J. Opt. A*, Vol. 1, pp.490-194.

27 Bennink, R.S., Yoon, Y-K. and Boyd, R.W. (1999) 'Accessing the optical nonlinearity of metals with metal-dielectric photonic bandgap structures', *Opt. Lett.*, Vol. 24, pp.1416–1418.

28 Dolgova, T.V., Madikovski, A.I., Martemyanov, M.G., Marovsky, G., Mattei, G., Schuhmacher, D., Yakovlev, V.A., Fedyanin, A.A. and Aktsipetrov, O.A. (2001) 'Giant second harmonic generation in microcavities based on porous silicon photonic crystals', *Jetp Lett.*, Vol. 73, pp.6–9.

29 Andreev, A.V., Balakin, A.V., Ozheredov, I.A., Shkurinov, A.P., Masselin, P., Mouret, G. and Boucher, D. (2000) 'Compression of femtosecond laser pulses in thin one-dimensional photonic crystals', *Phys. Rev. E*, Vol. 53, p.016602.

30 Scalora, M., Dowling, J.P., Bowden, C.M. and Bloemer, M.J. (1994) 'Optical limiting and switching of ultrashort pulses in nonlinear photonic band gap materials', *Phys. Rev. Lett.*, Vol. 73, pp.1368–1371.

31 Lan, S., Nishikawa, S. and Wada, O. (2001) 'Leveraging deep photonic band gaps in photonic crystal impurity bands', *Appl. Phys. Lett.*, Vol. 78, pp.2101–2103.

32 Lei, X-Y., Li, H., Ding, F., Zhang, W. and Ming, N-B. (1997) 'Novel application of a perturbed photonic crystal: high-quality filter', *Appl. Phys. Lett.*, Vol. 71, pp.2889–2891.

33 Qiao, F., Zhang, C., Wan, J. and Zi, J. (2000) 'Photonic quantum-well structures: multiple channelled filtering phenomena', *Appl. Phys. Lett.*, Vol. 77, pp.3698–3700.

34 Dowling, J.P., Scalora, M., Bloemer, M.J. and Bowden, C.M. (1994) 'The photonic band edge laser: a new approach to gain enhancement', *J. Appl. Phys.*, Vol. 75, pp.1896–1899.

35 Tocci, M.D., Scalora, M., Bloemer, M.J., Dowling, J.P. and Bowden, C.M. (1996) 'Measurement of spontaneous emission enhancement near the one-dimensional photonic band edge of semiconductor heterostructures', *Phys. Rev. A*, Vol. 53, pp.2799–2803.

36 Giorgis, F. (2000) 'Optical microcavities based on amorphous silicon-nitride Fabry-Perot structures', *Appl. Phys. Lett.,* Vol. 77, pp.522–524.

37 Serpenguzel, A. and Tanriseven, S. (2000) 'Controlled photoluminescence in amorphous-silicon-nitride microcavities', *Appl. Phys. Lett.,* Vol. 78, pp.1388–1390.

38 Bayindir, M., Tanriseven, S., Aydinli, A. and Ozbay, E. (2001) 'Strong enhancement of spontaneous emission in amorphous-silicon-nitride photonic crystal based coupled-microcavity structures', *Appl. Phys. A: Material Science Process*, Vol. 73, p.125.

39 Bayindir, M., Tanriseven, S. and Ozbay, E. (2001) 'Propagation of light through localized coupled-cavity modes in one-dimensional photonic band gap structures', *Appl. Phys. A: Material Science Process*, Vol. 72, pp.117–119.

40 Fan, S.H., Villeneuve, P.R., Joannopoulos, J.D. and Schubert, E.F. (1997) 'High extraction efficiency of spontaneous emission from slabs of photonic crystals', *Phys. Rev. Lett.*, Vol. 78, pp.3294–3297.

41 Boroditsky, M., Krauss, T.F., Coccioli, R., Vrijen, R., Bhat, R. and Yablonovitch, E. (1999) 'Light extraction from optically pumped light-emitting diode by thin-slab photonic crystals', *Appl. Phys. Lett.*, Vol. 75, pp.1036–1038.

42 Loncar, M., Yoshie, T., Scherer, A., Gogna, P. and Qiu, P. (2002) 'Low-threshold photonic crystal laser', *Appl. Phys. Lett.*, Vol. 81, p.2680.

43 Ryu, H.Y., Park, H.G. and Lee, Y.H. (2002) 'Two-dimensional photonic crystal semiconductor lasers: computational design, fabrication and characterization', *IEEE J. Sel. Top. Quant. Elect.*, Vol. 8, pp.891–908.

44 Yablonovitch, E., Gmitter, T.J., Meade, R.D., Rappe, A.M., Brommer, K.D. and Joannopoulos, J.D. (1991) 'Donor and acceptor modes in photonic band structure', *Phys. Rev. Lett.,* Vol. 67, pp.3380–3383.

45 Pavesi, L., Panzarini, G. and Andreani, L.C. (1998) 'All-porous silicon-coupled microcavities: experiment versus theory', *Phys. Rev. B*, Vol. 58, pp.15794–15800.

46 Stanley, R.P., Houdre, R., Oesterle, U., Ilegems, M. and Weisbuch, C. (1994) 'Coupled semiconductor microcavities', *Appl. Phys. Lett.*, Vol. 65, pp.2093–2095.

47 Hu, S.Y., Hegblom, E.R. and Coldren, L.A. (1997) 'Coupled-cavity resonant photodetectors for high-performance wavelength demultiplexing applications', *Appl. Phys. Lett.*, Vol. 71, pp.178–180.

48 Harrison, W.A. (1980) *Electronic Structure and the Properties of Solids*, W H Freeman & Co., San Francisco.

49 De Sterke, C.M. (1998) 'Superstructure gratings in the tight-binding approximation', *Phys. Rev. E*, Vol. 57, pp.3502–3509.

50 Stefanou, N. and Modinos, A. (1998) 'Impurity bands in photonic insulators', *Phys. Rev. B*, Vol. 57, pp.12127–12133.

51 Lidorikis, E., Sigalas, M.M., Economou, E.N. and Soukoulis, C.M. (1998) 'Tight-binding parametrization for photonic band gap materials', *Phys. Rev. Lett.*, Vol. 81, pp.1405–1408.

52 Mukaiyama, T., Takeda, K., Miyazaki, H., Jimba, Y. and Kuwata-Gonokami, M. (1999) 'Tight-binding photonic molecule modes of resonant bispheres', *Phys. Rev. Lett.*, Vol. 82, pp.4623–4626.

53 Yariv, A., Xu, Y., Lee, R.K. and Scherer, A. (1999) 'Coupled-resonator optical waveguide: a proposal and analysis', *Opt. Lett.*, Vol. 24, pp.711–713.

54 Bayindir, M., Temelkuran, B. and Ozbay, E. (2000) 'Tight-binding description of the coupled defect modes in three-dimensional photonic crystals', *Phys. Rev. Lett.*, Vol. 84, pp.2140–2143.

55 Bayindir, M., Temelkuran, B. and Ozbay, E. (2000) 'Propagation of photons by hopping: a waveguiding mechanism through localized coupled-cavities in three-dimensional photonic crystals', *Phys. Rev. B*, Vol. 61, pp.R11855–R11858.

56 Aydinli, A., Serpenguzel, A. and Vardar, D. (1996) 'Visible photoluminescence from low temperature deposited hydrogenated amorphous silicon nitride', *Solid State Commun.*, Vol. 98, p.273.

57 Bayindir, M. and Ozbay, E. (2000) 'Heavy photons at coupled-cavity waveguide band edges in a three-dimensional photonic crystal', *Phys. Rev. B*, Vol. 62, pp.R2247–R2250.

58 Bayindir, M., Kural, C. and Ozbay, E. (2001) 'Coupled optical microcavities in one-dimensional photonic bandgap structures', *J. Opt. A*, Vol. 3, pp.S184–S189.

59 Yablonovitch, E. (1987) 'Inhibited spontaneous emission in solid-state physics and electronics', *Phys. Rev. Lett.*, Vol. 58, p.2059.

60 Vredenberg, A.M., Hunt, N.E.J., Schubert, E.F., Jacobson, D.C., Poate, J.M. and Zydzik, G.J. (1993) 'Controlled atomic spontaneous emission from Er^{3+} in a transparent Si/SiO_2 microcavity', *Phys. Rev. Lett.*, Vol. 71, p.517.

61 John, S. and Quang, T. (1994) 'Spontaneous emission near the edge of a photonic band gap', *Phys. Rev. A*,, Vol. 50, p.1764.

62 Pavesi, L., Mazzoleni C., Tredicucci A. and Pellegrini V. (1995) 'Controlled photon emission in porous silicon microcavities', *Appl. Phys. Lett.*, Vol. 67, p.3280.

63 Serpenguzel, A., Aydinli, A., Bek, A. and Gure, M. (1998) 'Visible photoluminescence from planar amorphous silicon nitride microcavities', *J. Opt. Soc. Am. B*, Vol. 15, p.2706.

64 Lee, R.K., Painter, O.J., D'Urso, B., Scherer, A. and Yariv, A. (1999) 'Measurement of spontaneous emission from a two-dimensional photonic band gap defined microcavity at near-infrared wavelengths', *Appl. Phys. Lett.*, Vol. 74, p.1522.

65 Boroditsky, M., Vrijen, R., Krauss, T.F., Coccioli, R., Bhat, R. and Yablonovitch E. (1999) 'Spontaneous emission extraction and Purcell enhancement from thin-film 2-D photonic crystals'**,** *IEEE J. Lightw. Tech.*, Vol. 17, p.2096.

66 Lopez, H.A. and Fauchet, P.M. (2000) 'Erbium emission from porous silicon one-dimensional photonic band gap structures', *Appl. Phys. Lett.*, Vol. 77, p.3704.

67 Dukin, A.A., Feoktistov, N.A, Golubev, V.G., Medvedev, A.V., Pevtsov, A.B. and Sel'kin, A.V. (2000) 'Optical properties of a Fabry–Pérot microcavity with Er-doped hydrogenated amorphous silicon active layer', *Appl. Phys. Lett.*, Vol. 77, p.3009.

68 Veselago, V.G. (1968) 'The electrodynamics of substances with simultaneously negative values of ε and μ', *Sov. Phys. Uspekhi*, Vol. 10, pp.509–514.

69 Pendry, J.B., Holden, A.J., Stewart, W.J. and Youngs, I. (1996) 'Extremely low frequency plasmons in metallic mesostructures', *Phys. Rev. Lett.*, Vol. 76, pp.4773–4776.

70   Pendry, J.B., Holden, A.J., Robins, D.J. and Stewart, W.J. (1999) 'Magnetism from conductors and enhanced nonlinear phenomena', *IEEE T. Microw. Theory*, Vol. 47, pp.2075–2084.

71   Smith, D.R., Padilla, W.J., Vier, D.C., Nemat-Nasser, S.C. and Schultz, S. (2000) 'Composite medium with simultaneously negative permeability and permittivity', *Phys. Rev. Lett.*, Vol. 84, pp.4184–4187.

72   Shelby, R.A., Smith, D.R. and Schultz, S. (2001) 'Experimental verification of a negative index of refraction', *Science*, Vo. 292, pp.77–79.

73   Smith, D.R., Schultz, S., Markos, P. and Soukoulis, C.M. (2002) 'Determination of effective permittivity and permeability of metamaterials from reflection and transmission coefficients', *Phys. Rev. B*, Vol. 65, p.195104.

74   Bayindir, M., Aydin, K., Ozbay, E., Markos, P. and Soukoulis, C.M. (2002) 'Transmission properties of composite metamaterials in free space', *Appl. Phys. Lett.*, Vol. 81, pp.120–122.

75   Markos, P. and Soukoulis, C.M. (2002) 'Transmission studies of left-handed materials', *Phys. Rev. B*, Vol. 65, p.033401.

76   Ziolkowski, R.W. and Heyman, E. (2001) 'Wave propagation in media having negative permittivity and permeability', *Phys. Rev. B*, Vol. 64, p.056625.

77   Valanju, P.M., Walser, R.M. and Valanju, A.P. (2002) 'Wave refraction in negative-index media: always positive and very inhomogeneous', *Phys. Rev. Lett.*, Vol. 88, p.187401.

78   Pokrovsky, A.L. and Efros, A.L. (2002) 'Electrodynamic of metallic photonic crystals and the problem of left handed materials', *Phys. Rev. Lett.*, Vol. 89, p.093901.

79   Notomi, M. (2000) 'Theory of light propagation in strongly modulated photonic crystals: refractionlike behavior in the vicinity of the photonic band gap', *Phys. Rev. B*, Vol. 62, pp.10696–10705.

80   Gralak, B., Enoch, S. and Tayeb, G. (2000) 'Anomalous refractive properties of photonic crystals', *J. Opt. Soc. Am. A*, Vol. 17, pp.1012–1020.

81   Luo, C., Johnson, S.G., Joannopoulos, J.D. and Pendry, J.B. (2002) 'All-angle negative refraction without negative effective index', *Phys. Rev. B*, Vol. 65, p.R201104.

82   Foteinopoulou, S., Economou, E.N., Soukoulis, C.M. (2003) 'Refraction in media with a negative refractive index', *Phys. Rev. Lett.*, Vol. 90, p.107402-1.

83   Pendry, J.B. (2000) 'Negative refraction makes a perfect lens', *Phys. Rev. Lett.*, Vol. 85, pp.3966–3969.

84   Hooft, G.W.'t (2001) 'Comment on 'Negative refraction makes a perfect lens'', *Phys. Rev. Lett.*, Vol. 87, p.249701.

85   Pendry, J. (2001) 'Pendry replies:', *Phys. Rev. Lett.*, Vol. 87, p.249702.

86   Williams, J.M. (2001) 'Some problems with negative refraction', *Phys. Rev. Lett.*, Vol. 87, p.249703.

87   Pendry, J. (2001) 'Pendry replies:', *Phys. Rev. Lett.*, Vol. 87, p.249704.

88   Garcia, N. and Nieto-Vesperinas, M. (2002) 'Left handed materials do not make a perfect lens', *Phys. Rev. Lett.*, Vol. 88, p.207403.

89   Luo, C., Johnson, S.G. and Joannopoulos, J.D. (2003) 'Subwavelength imaging in photonic crystals', *Phys. Rev. B*, Vol. 68, p.045115.